Sequence, infectivity and replication kinetics of SARS-CoV-2 isolated from COVID-19 patients in Canada

Arinjay Banerjee[1], Jalees A. Nasir[1], Patrick Budylowski[2], Lily Yip[3], Patryk Aftanas[3], Natasha Christie[2], Ayoob Ghalami[2], Kaushal Baid[1], Amogelang R. Raphenya[1], Jeremy A. Hirota[1], Matthew S. Miller[1], Mario Ostrowski[2], Robert A. Kozak[2,3], Andrew G. McArthur[1], Karen Mossman[1,*] and Samira Mubareka[2,3]

Affiliations:

[1]McMaster University, Hamilton, Ontario, Canada

[2]University of Toronto, Toronto, Ontario, Canada

[3]Sunnybrook Research Institute, Toronto, Ontario, Canada

*Corresponding author:

Dr. Karen Mossman

McMaster University

1280 Main St. W

Hamilton L8S 4L8, Canada

Email: mossk@mcmaster.ca

ABSTRACT

SARS-CoV-2 emerged in December 2019 in Wuhan, China and has since infected over 1.5 million people, of which over 107,000 have died. As SARS-CoV-2 spreads across the planet, speculations remain about the range of human cells that can be infected by SARS-CoV-2. In this study, we report the isolation of SARS-CoV-2 from two COVID-19 patients in Toronto, Canada. We determined the genomic sequences of the two isolates and identified single nucleotide changes in representative populations of our virus stocks. More importantly, we tested a wide range of human immune cells for productive infection with SARS-CoV-2. Here we confirm that human primary peripheral blood mononuclear cells (PBMCs) are not permissive to SARS-CoV-2. As SARS-CoV-2 continues to spread globally, it is essential to monitor small nucleotide polymorphisms in the virus and to continue to isolate circulating viruses to determine cell susceptibility and pathogenicity using *in vitro* and *in vivo* infection models.

Keywords: SARS-CoV-2, isolation, replication, immune cells, phylogenetics, COVID-19

TEXT

A new coronavirus, severe acute respiratory syndrome coronavirus 2 (SARS-CoV-2) emerged in December 2019 in Wuhan, China (1). SARS-CoV-2 has since spread to 185 countries and infected over 1.7 million people, of which over 107,000 have died (2). The first case of COVID-19 was detected in Toronto, Canada on January 23, 2020 (3). Multiple cases have since been identified across Canada. As SARS-CoV-2 spreads globally, the virus is likely to adapt and evolve. It is critical to isolate SARS-CoV-2 viruses to characterize their ability to infect and replicate in multiple human cell types and to determine if the virus is evolving in its ability to infect human cells and cause severe disease. Isolating the virus also provides us with the

46 opportunity to share the virus with other researchers to facilitate the development and testing of
47 diagnostics, drugs and vaccines.
48
49 In this study, we describe how we isolated and determined the genomic sequence of SARS-CoV-
50 2 from two Toronto COVID-19 patients (SARS-CoV-2/SB2 and SARS-CoV-2/SB3-TYAGNC).
51 In addition, we studied the replication kinetics of SARS-CoV-2/SB3-TYAGNC in human
52 structural and immune cells. Importantly, we report that although a human lung cell line
53 supported SARS-CoV-2 replication, the virus did not propagate in any of the tested immune cell
54 lines or primary human immune cells. Interestingly, although we did not observe a productive
55 infection in $CD4^+$ primary T cells, we observed virus-like particles in these cells by electron
56 microscopy. Our data shed light on a wider range of human cells that may or may not be
57 permissive for SARS-CoV-2 replication and our studies strongly suggest that a broad range of
58 human immune cells are unlikely to support SARS-CoV-2 infection in COVID-19 patients.
59 **METHODS**
60 **Cells**
61 Vero E6 cells (African green monkey cells; ATCC, https://www.atcc.org) were maintained in
62 Dulbecco's modified Eagle's media (DMEM) supplemented with 10% fetal bovine serum (FBS;
63 Sigma-Aldrich, https://www.sigmaaldrich.com), 1x L-Glutamine and Penicillin/Streptomycin
64 (Pen/Strep; Corning, https://ca.vwr.com). Calu-3 cells (human lung adenocarcinoma derived;
65 ATCC, https://www.atcc.org) were cultured as previously mentioned (4). THF cells (human
66 telomerase life-extended cells) were cultured as previously mentioned (5). THP-1 cells
67 (monocytes; ATCC, https://www.atcc.org) were cultured in RPMI media (Gibco,
68 https://www.thermofisher.com) supplemented with 10% FBS, 2mM L-glutamine, 1x

69 Penicillin/streptomycin and 0.05 mM beta-mercaptoethanol. THP-1 cells were differentiated into
70 macrophages and dendritic cells using 50 ng/ml GM-CSF (R&D Systems,
71 https://www.rndsystems.com) + 50 ng/ml M-CSF (R&D Systems, https://www.rndsystems.com)
72 and 50 ng/ml GM-CSF + 500 U/ml IL-4 (Biolegend, https://www.biolegend.com), respectively.
73 PBMCs from healthy donors (n=2; OM8066 and OM8067) were purified into $CD4^+$, $CD8^+$,
74 $CD19^+$, monocytes and others ($CD4^-$ $CD8^-$ $CD19^-$ cells) using CD4 negative selection kit
75 (STEMCELL Technologies, https://www.stemcell.com), CD8 positive selection kit
76 (STEMCELL Technologies, https://www.stemcell.com), PE positive selection kit (STEMCELL
77 Technologies, https://www.stemcell.com) and Monocyte negative selection kit (STEMCELL
78 Technologies, https://www.stemcell.com), respectively. For purity of cell types, see
79 supplementary figure 1. $CD4^+$, $CD8^+$, $CD19^+$ and $CD4^-$ $CD8^-$ $CD19^-$ cells were resuspended in
80 R-10 media (RPMI + 2 mM L-glutamine + 10% FBS + Penicillin/streptomycin) + 20 U/ml IL-2
81 (Biolegend, https://www.biolegend.com). Primary monocytes were resuspended in R-10 media.
82 Work with PBMCs was approved by the Research Ethics Boards of St. Michael's Hospital and
83 the University of Toronto (REB 20-044).

84 **Virus isolation and quantification**

85 Vero E6 cells were seeded at a concentration of $3x10^5$ cells/well in a 6-well plate. Next day,
86 200 µl of mid-turbinate swabs, collected from two COVID-19 patients in viral transport media
87 was mixed with 200 µl of DMEM containing 16 µg/ml TPCK-treated trypsin. The cells were
88 infected with the inoculum for 1 hr. Next, the inoculum was replaced with DMEM containing
89 2% FBS and 8 µg/ml TPCK-treated trypsin. The cells were observed daily under a light
90 microscope. Supernatant from the cells were used to determine virus titres ($TCID_{50}$/ml) using
91 Spearman and Karber's method (6, 7) as outlined previously (8).

92 **Quantitative real time PCR**

93 To detect SARS-CoV-2 in cell culture supernatant, 140 uL of supernatant was removed and
94 detection of viral nucleic acids was performed by RT-PCR using an adaptation of Corman *et*
95 *al.'s* protocol (9). Briefly, viral RNA was extracted from infected cells using QIAamp viral RNA
96 kit (Qiagen, https://www.qiagen.com) according to manufacturer's instructions. The RT-PCR
97 reactions were carried out using Luna Universal qPCR Master Mix (New England Biolabs,
98 https://www.neb.ca) according to manufacturer's instructions. Two separate gene targets were
99 used for detection, the 5' untranslated region (UTR) and the envelope (E) gene. Primers and
100 probes used were: 5'-UTR For: GTTGCAGCCGATCATCAGC; 5'-UTR Rev:
101 GACAAGGCTCTCCATCTTACC; 5'-UTR probe: FAM-
102 CGGTCACACCCGGACGAAACCTAG-BHQ-1; E-gene For:
103 ACAGGTACGTTAATAGTTAATAGCGT; E-gene Rev: ATATTGCAGCAGTACGCACACA;
104 E-gene probe: CAL Fluor Orange 560-ACACTAGCCATCCTTACTGCGCTTCG-BHQ-1. The
105 cycling conditions were: 1 cycle of denaturation at 60°C for 10 minutes then 95°C for 2 minutes
106 followed by 44 amplification cycles of 95°C for 10s and 60°C for 15s. Analysis was performed
107 using the Rotor-Gene Q software (Qiagen, https://www.qiagen.com) to determine cycle
108 thresholds (Ct).

109 **Electron Microscopy**

110 Samples were fixed in 10% neutral buffered formalin (Sigma-Aldrich,
111 https://www.sigmaaldrich.com/) for 1 hr. Pellets were washed with 0.1 M phosphate buffer (pH
112 7.0) and post-fixed with 1% osmium tetroxide in 0.1 M phosphate buffer (pH 7.0) for 1 hr.
113 Pellets were washed with distilled water and en-bloc stained with 2% uranyl acetate in distilled
114 water for 2 hrs. Pellets were washed with distilled water and dehydrated in an ethanol series.

115 Pellets were infiltrated with Embed 812/Araldite resin and cured at 65 degrees for 48 hrs. Resin
116 blocks were trimmed, polished and 90 nm thin sections were ultramicrotomed (Leica Reichert
117 Ultracut E, https://www.leica-microsystems.com) and mounted on TEM grids. Thin sections
118 were stained with 5% uranyl acetate and 5% lead citrate. Sections were imaged using
119 Transmission Electron Microscopy (ThermoFisher Scientific Talos L120C,
120 https://www.thermofisher.com) using a LaB6 filament at 120kV. 10 fields per cell type were
121 scanned. Each field was imaged with different magnifications at 2600x, 8500x, 17500x and
122 36000x.

123 **Flowcytometry**

124 100μL (400,000 cells) of primary $CD4^+$, $CD8^+$, $CD19^+$ and monocytes were washed with 1 ml of
125 phosphate buffered saline (PBS) and spun at 500 g for 5 minutes. The cells were resuspended in
126 100 μL of Live/Dead Violet (ThermoFisher Scientific, https://www.thermofisher.com) as per
127 manufacturer's recommendation and diluted 1:1000 in PBS. Cells were incubated at 4°C for 30
128 minutes. Next, cells were washed with 1 ml of FACS buffer (in-house reagent) and spun at 500 g
129 for 5 minutes. Cells were then stained with 100 μL of their respective stains (αCD4-FITC,
130 αCD8-FITC, αCD19-FITC, αCD14-APC; Biolegend, https://www.biolegend.com) at a
131 concentration of 1μg/mL for 30 min at 4°C. After staining, the cells were washed with 1mL of
132 FACS Buffer and spun at 500 g for 5 minutes. Extra aliquots of cells were left unstained, which
133 were also spun at 500g for 5 minutes. The pellets were resuspended in 100 μL of 1%
134 paraformaldehyde (PFA; ThermoFisher Scientific, https://www.thermofisher.com) and analyzed.
135 Samples were run on the BD LSR Fortessa X20 (BD, https://www.bdbiosciences.com). Cells
136 were gated on Live/Dead negative to exclude debris and dead cells and were then gated on their
137 respective cell surface markers to assess purity.

138 **Sequencing**

139 RNA was extracted from the supernatant of Vero E6 cells that were inoculated with clinical
140 specimens after 1 passage using the QIAamp Viral RNA Mini kit (Qiagen,
141 https://www.qiagen.com/us/) without addition of carrier RNA. dsDNA for sequencing library
142 preparation was synthesized using the Liverpool SARS-CoV-2 amplification protocol (10). Two
143 100 µM primer pools were prepared by combining primer pairs in an alternating fashion to
144 prevent amplification of overlapping regions in a single reaction. In a PCR tube, 1µL Random
145 Primer Mix (ProtoScript II First Strand cDNA Synthesis Kit, New England Biolabs,
146 https://www.neb.ca) was added to 7 µL extracted RNA and denatured on SimpliAmp thermal
147 cycler (ThermoFisher Scientific, https://www.thermofisher.com) at 65°C for 5 min and then
148 incubated on ice. 10 µL 2X ProtoScript II Reaction Mix and 2 µL 10X ProtoScript II Enzyme
149 Mix were then added to the denatured sample and cDNA synthesis performed using the
150 following conditions: 25°C for 5 min, 48°C for 15 min and 80°C for 5 min. After cDNA
151 synthesis, in a new PCR tube 2.5 µL cDNA was combined with 12.5 µL Q5 High-Fidelity 2X
152 Master Mix (NEB, Ipswich, USA), 8.8 µL nuclease free water (ThermoFisher Scientific,
153 https://www.thermofisher.com), and 1.125 µL of 100 µM primer pool #1 or #2. PCR cycling was
154 then performed as follows: 98°C for 30 sec followed by 40 cycles of 98°C for 15 sec and 65°C
155 for 5 min.

156

157 All PCR reactions were purified using RNAClean XP (Beckman Coulter,
158 https://www.beckmancoulter.com) at 1.8x bead to amplicon ratio and eluted in 30 µL. 2 µL of
159 amplified material was quantified using a Qubit 1X dsDNA (ThermoFisher Scientific,
160 https://www.thermofisher.com) following the manufacturer's instructions. Illumina sequencing

161 libraries were prepared using Nextera DNA Flex Library Prep Kit and Nextera DNA CD Indexes
162 (Illumina, https://www.illumina.com) according to manufacturer's instructions. Paired-end 150
163 bp sequencing was performed for each library on a MiniSeq with the 300-cycle mid-output
164 reagent kit (Illumina, https://www.illumina.com), multiplexed with targeted sampling of ~40,000
165 clusters per library. Sequencing reads from pool #1 and pool #2 were combined (as R1 and R2),
166 amplification primer sequences removed using cutadapt (version 1.18) (11), and Illumina adapter
167 sequences were removed and low quality sequences trimmed or removed using Trimmomatic
168 (version 0.36) (12). Final sequence quality and confirmation of adapter/primer trimming were
169 confirmed by FASTQC (version 0.11.5) (13). SARS-CoV-2 genome sequences were assembled
170 using UniCycler (version 0.4.8; default settings, except for --mode conservative) (14) and
171 assembly statistics generated by QUAST (version 5.0.2) (15). Sequencing depth and
172 completeness of coverage of the assembled genomes was additionally assessed by Bowtie2
173 (version 2.3.4.1) (16) alignment of the sequencing reads against the assembled contigs and
174 stastistics generated by ngsCAT (version 0.1) (17). Sequence variation in the assembled genomes
175 was assessed by BLASTN against SARS-CoV-2 genome sequences available in GenBank as
176 well as BreSeq (version 0.35.0) (18) analysis relative to GenBank entry MN908947.3 (first
177 genome sequence reported from the original Wuhan outbreak, China).
178
179 **RESULTS**
180 To facilitate virus isolation, we collected mid-turbinate swabs from two COVID-19 patients in
181 Toronto, Canada and transported the swabs in viral transport media to a high containment level 3
182 facility. We inoculated Vero E6 cells with the samples and observed for cytopathic effects (CPE)
183 daily. Seventy-two hours post infection (hpi), cells inoculated with both samples displayed

184 extensive CPE, relative to mock inoculated cells (Figure 1, panel A). We collected 200 uL of cell
185 culture supernatant and re-infected a fresh layer of Vero E6 cells. Twenty-four hours post
186 infection, both wells containing cells that were re-inoculated displayed extensive CPE (Figure 1,
187 panel B). We extracted viral RNA from the supernatant and confirmed the presence of SARS-
188 CoV-2 using a diagnostic quantitative real-time PCR assay (qPCR; Figure 1, panel C). We also
189 confirmed the presence of coronavirus-like particles in infected Vero E6 cells by electron
190 microscopy (Figure 1, panel D).
191
192 Next, we performed genome sequencing of both isolates, generating nearly complete genome
193 sequences with 7500-8000 fold coverage and ~94% completeness, with only ~260 bp and ~200
194 bp at the 5' and 3' termini undetermined (Table 1). Both shared synonymous and non-
195 synonymous substitutions with those independently observed in direct sequencing of clinical
196 isolates (Table 1; Mubareka & McArthur, unpublished). SARS-CoV-2/SB2 additionally
197 contained a non-synonymous substitution at position 2832 (K856R in ORF1ab polyprotein) and
198 three regions with mutations or a deletion supported by a minority of sequencing reads, while
199 SARS-CoV-2/SB3-TYAGNC only had an additional synonymous substitution in ORF1ab
200 polyprotein (Y925Y) plus a minority of sequencing reads supporting another synonymous
201 substitution in the ORF3a protein (I7I). As such, SARS-CoV-2/SB3-TYAGNC was used for
202 subsequent studies as best representative of patient infections. Raw sequencing reads for each
203 isolate are available in NCBI BioProject PRJNA624792. Only sequencing reads that aligned by
204 Bowtie2 to the MN908947.3 SARS-CoV-2 genome were included in the deposited sequence
205 files.
206

207 To determine the replication kinetics of SARS-CoV-2 in human structural and immune cells, we
208 infected Calu-3 (lung adenocarcinoma epithelial), THF (telomerase life extended human
209 fibroblasts), Vero E6 (African green monkey kidney epithelial), THP-1 (monocytes and
210 differentiated macrophages and dendritic cells) and primary peripheral blood mononuclear cells
211 (PBMCs) from healthy human donors ($CD4^+$, $CD8^+$, $CD19^+$, monocytes and other PBMCs;
212 Supplementary Figure S1) with a multiplicity of infection (MOI) of 0.01. We monitored virus
213 replication over a period of 72 hours in the cell lines (Figure 2). We also determined virus
214 replication in PBMCs from healthy donors over a period of 48 hours (Figure 2). SARS-CoV-2
215 propagated to high titres in Vero E6 and Calu-3 cells (Figure 2). SARS-CoV-2 did not replicate
216 efficiently in THF cells (Figure 2). Interestingly, human immune cell lines and primary PBMCs
217 from healthy donors did not support SARS-CoV-2 replication (Figure 2)
218
219 To further support virus replication data, we imaged infected human structural and immune cells
220 using electron microscopy (Figure 3). We scanned 10 different fields per cell type, each using
221 four different magnifications of 2600x, 8500x, 17500x and 36000x to determine if the cell
222 populations contained virus-like particles. Virus-like particles were detected in 7/10 fields in
223 Vero E6 cells and 8/10 fields in Calu-3 cells (Figure 3, panels A and B). Interestingly, we also
224 detected virus-like particles in 2/10 fields in primary $CD4^+$ T cells (Figure 3, panel C). We did
225 not observe any virus-like particles in other human immune cells that were experimentally
226 infected with SARS-CoV-2 (Figure 3, panels D-J).
227
228 **DISCUSSION**

229 In this study, we report the isolation of two replication competent SARS-CoV-2 isolates from
230 COVID-19 patients in Canada. Although we used TPCK-treated trypsin to enhance infection
231 using clinical specimens (Figure 1, panel A), subsequent infection and virus replication did not
232 require any additional TPCK-treated trypsin (Figure 1, panel B). We sequenced both isolates to
233 confirm that they were reflective of isolates infecting patients worldwide, selecting SARS-CoV-
234 2/ SB3-TYAGNC for experimental investigation as its sequencing produced less minority
235 sequencing reads (Table 1).
236
237 SARS-CoV caused the 2004 pandemic of SARS. SARS-CoV can infect structural (19) and
238 immune cell lines (20) from humans *in vitro*. We infected a wide range of human cell
239 populations with SARS-CoV-2/SB3-TYAGNC to identify cell types that can support productive
240 infection of SARS-CoV-2. Both Vero E6 and Calu-3 cells supported virus replication to high
241 titres (Figure 2), as reported in other recent studies (21, 22). hTERT life-extended human
242 fibroblast cells (THF) did not support virus replication (Figure 2). In addition, human immune
243 cell populations, including cell lines (THP-1) and primary cells (PBMCs) did not support
244 productive SARS-CoV-2 replication (Figure 2). Interestingly, although primary $CD4^+$ T cells did
245 not support productive virus replication, we observed virus-like particles in these cells by
246 electron microscopy (Figure 3, panel C). This is consistent with a recent report by Wang and
247 colleagues where they demonstrated that human T cell lines could be infected with SARS-CoV-2
248 (23). However, the study by Wang *et al.* did not quantify virus titres in the supernatant from
249 infected cells. In our study, we could not detect any replication competent virus in the
250 supernatant that was collected from SARS-CoV-2 infected $CD4^+$ T cells (Figure 3).
251

252 In this study, we show that primary human T cells ($CD4^+$ and $CD8^+$) do not support productive
253 virus replication. However, our electron micrographs demonstrate that SARS-CoV-2 likely
254 replicates in $CD4^+$ T cells, but the replication cycle is likely terminated prior to virus maturation
255 and egress. Thus, more work is needed to fully identify the susceptibility and permissivity of
256 $CD4^+$ T cells to SARS-CoV-2.
257
258 **ACKNOWLEDGEMENTS**
259 We would like to acknowledge Lindsey Fiddes' help with electron microscopy. SARS-CoV-2
260 Liverpool protocol genome amplification primer sequences were generously shared by Public
261 Health England.
262
263 This study was supported by a Canadian Institutes of Health Research (CIHR) grant to principal
264 applicant K.M. and Co-Applicants A.B., A.G.M., M.S.M. and S.M. A.B. is funded by the
265 Natural Sciences and Engineering Research Council of Canada (NSERC). J.A.N. was supported
266 by funds from the Comprehensive Antibiotic Resistance Database. B.P.A. and A.R.R. were
267 supported by Canadian Institutes of Health Research (CIHR) funding (PJT-156214 to A.G.M.).
268 Computer resources were supplied by the McMaster Service Lab and Repository computing
269 cluster, funded in part by grants to A.G.M. from the Canadian Foundation for Innovation.
270 Additional cloud computing needs were funded by the Comprehensive Antibiotic Resistance
271 Database. . J.A.H. is supported by the Canada Research Chairs Program and an Ontario Early
272 Career Researcher Award.
273
274

275 **REFERENCES**

276 1. Zhou P, Yang XL, Wang XG, Hu B, Zhang L, Zhang W, et al. A pneumonia outbreak
277 associated with a new coronavirus of probable bat origin. Nature. 2020 Feb 3.

278 2. Dong E, Du H, Gardner L. An interactive web-based dashboard to track COVID-19 in
279 real time. The Lancet Infectious Diseases. 2020.

280 3. Marchand-Senecal X, Kozak R, Mubareka S, Salt N, Gubbay JB, Eshaghi A, et al.
281 Diagnosis and Management of First Case of COVID-19 in Canada: Lessons applied from SARS.
282 Clin Infect Dis. 2020 Mar 9.

283 4. Aguiar JA, Huff RD, Tse W, Stampfli MR, McConkey BJ, Doxey AC, et al.
284 Transcriptomic and barrier responses of human airway epithelial cells exposed to cannabis
285 smoke. Physiol Rep. 2019 Oct;7(20):e14249.

286 5. Banerjee A, Zhang X, Yip A, Schulz KS, Irving AT, Bowdish D, et al. Positive Selection
287 of a Serine Residue in Bat IRF3 Confers Enhanced Antiviral Protection. iScience. 2020 Mar
288 2;23(3):100958.

289 6. Hamilton MA, Russo RC, Thurston RV. Trimmed Spearman-Karber method for
290 estimating median lethal concentrations in toxicity bioassays. Environmental Science &
291 Technology. 1977;11(7):714-9.

292 7. Spearman C. The Method of “Right and Wrong Cases” (Constant Stimuli) without
293 Gauss’s Formula. Br J Psychol. 1908;2:227-42.

294 8. Banerjee A, Falzarano D, Rapin N, Lew J, Misra V. Interferon Regulatory Factor 3-
295 Mediated Signaling Limits Middle-East Respiratory Syndrome (MERS) Coronavirus
296 Propagation in Cells from an Insectivorous Bat. Viruses. 2019 Feb 13;11(2).

297 9. Corman VM, Landt O, Kaiser M, Molenkamp R, Meijer A, Chu DKW, et al. Detection of
298 2019 novel coronavirus (2019-nCoV) by real-time RT-PCR. Euro Surveill. 2020 Jan;25(3).
299 10. Quick J, Grubaugh ND, Pullan ST, Claro IM, Smith AD, Gangavarapu K, et al. Multiplex
300 PCR method for MinION and Illumina sequencing of Zika and other virus genomes directly
301 from clinical samples. Nat Protoc. 2017 Jun;12(6):1261-76.
302 11. Martin M. Cutadapt removes adapter sequences from high-throughput sequencing reads.
303 EMBnetjournal. 2011;17(1).
304 12. Bolger AM, Lohse M, Usadel B. Trimmomatic: a flexible trimmer for Illumina sequence
305 data. Bioinformatics. 2014 Aug 1;30(15):2114-20.
306 13. Andrew S. FastQC: A Quality Control Tool for High Throughput Sequence Data
307 [Online]. 2010 [cited 2020 April 09]; Available from:
308 http://www.bioinformatics.babraham.ac.uk/projects/fastqc/
309 14. Wick RR, Judd LM, Gorrie CL, Holt KE. Unicycler: Resolving bacterial genome
310 assemblies from short and long sequencing reads. PLoS Comput Biol. 2017 Jun;13(6):e1005595.
311 15. Gurevich A, Saveliev V, Vyahhi N, Tesler G. QUAST: quality assessment tool for
312 genome assemblies. Bioinformatics. 2013 Apr 15;29(8):1072-5.
313 16. Langmead B, Salzberg SL. Fast gapped-read alignment with Bowtie 2. Nat Methods.
314 2012 Mar 4;9(4):357-9.
315 17. Lopez-Domingo FJ, Florido JP, Rueda A, Dopazo J, Santoyo-Lopez J. ngsCAT: a tool to
316 assess the efficiency of targeted enrichment sequencing. Bioinformatics. 2014 Jun
317 15;30(12):1767-8.
318 18. Deatherage DE, Barrick JE. Identification of mutations in laboratory-evolved microbes
319 from next-generation sequencing data using breseq. Methods Mol Biol. 2014;1151:165-88.

320 19. Kaye M. SARS-associated coronavirus replication in cell lines. Emerg Infect Dis. 2006
321 Jan;12(1):128-33.
322 20. Yen YT, Liao F, Hsiao CH, Kao CL, Chen YC, Wu-Hsieh BA. Modeling the early events
323 of severe acute respiratory syndrome coronavirus infection in vitro. J Virol. 2006
324 Mar;80(6):2684-93.
325 21. Harcourt J, Tamin A, Lu X, Kamili S, Sakthivel SK, Murray J, et al. Severe Acute
326 Respiratory Syndrome Coronavirus 2 from Patient with 2019 Novel Coronavirus Disease, United
327 States. Emerg Infect Dis. 2020 Mar 11;26(6).
328 22. Matsuyama S, Nao N, Shirato K, Kawase M, Saito S, Takayama I, et al. Enhanced
329 isolation of SARS-CoV-2 by TMPRSS2-expressing cells. Proc Natl Acad Sci U S A. 2020 Mar
330 31;117(13):7001-3.
331 23. Wang X, Xu W, Hu G, Xia S, Sun Z, Liu Z, et al. SARS-CoV-2 infects T lymphocytes
332 through its spike protein-mediated membrane fusion. Cellular & Molecular Immunology. 2020.
333
334
335
336
337
338
339
340
341
342

343 **FIGURES AND FIGURE LEGENDS**

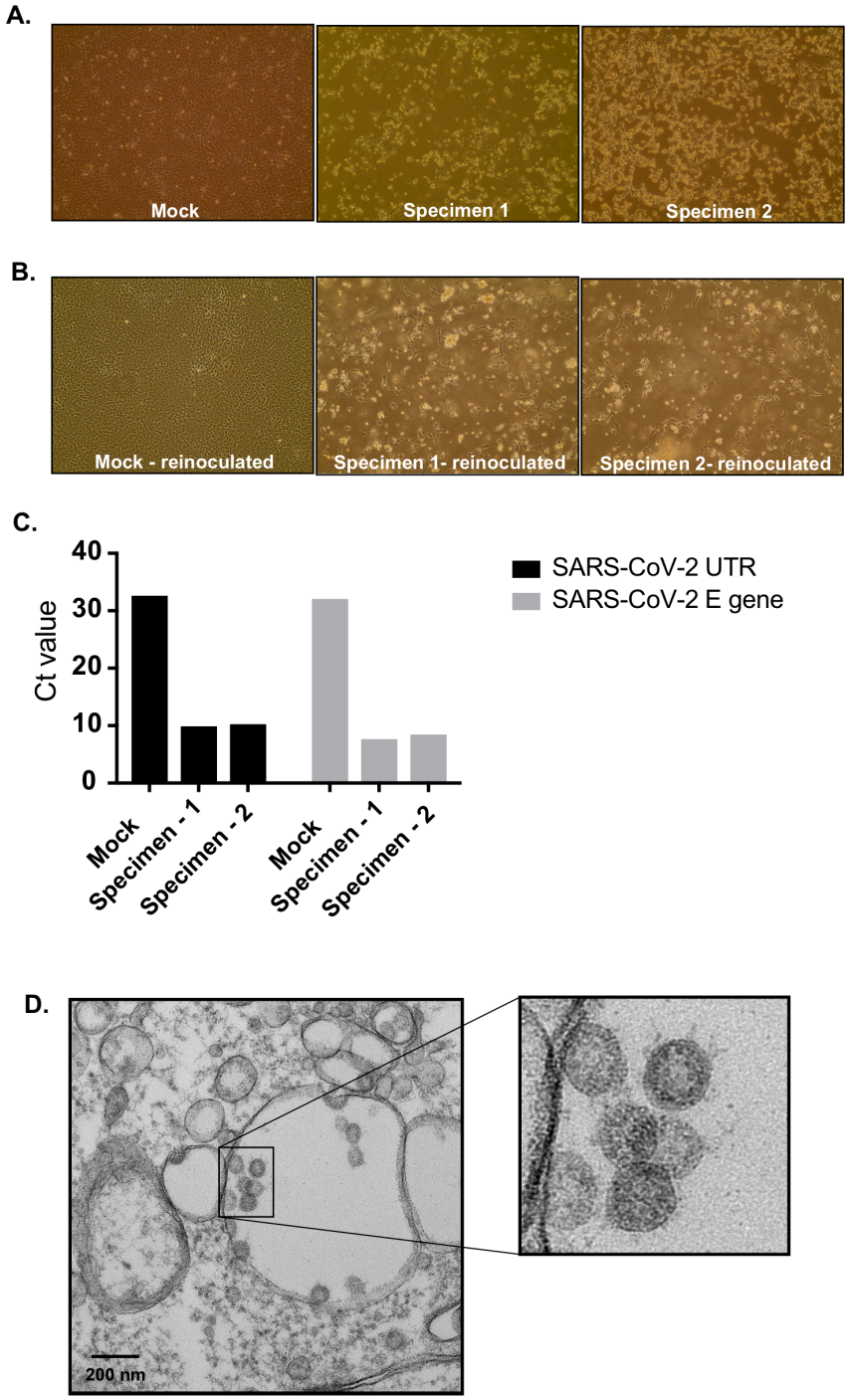

344

345 **Figure 1. Isolating SARS-CoV-2 from COVID-19 patients.** (A) Vero E6 cells were mock

346 inoculated or inoculated with mid-turbinate clinical specimens from COVID-19 patients. Cells

347 were incubated for 72 hours and observed for cytopathic effect (CPE) under a light microscope.

348 (B) To determine if supernatant from Vero E6 cells that were mock inoculated or inoculated with
349 clinical specimens contained replication competent virus, we re-inoculated fresh monolayer of
350 Vero E6 cells and observed cells under a light microscope for CPE after 24 hours. (C)
351 Quantitative real time PCR to detect SARS-CoV-2 5'- untranslated region (UTR) and envelope
352 (E) gene in RNA extracted from supernatant that was collected from Vero E6 cells that were
353 mock infected or infected with COVID-19 clinical specimens for 72 hours. (D) Electron
354 micrograph of Vero E6 cells that were re-infected for 48 hours with supernatant that was
355 collected from Vero E6 cells infected with clinical specimens. Insert – zoomed image of
356 coronavirus-like particles.
357

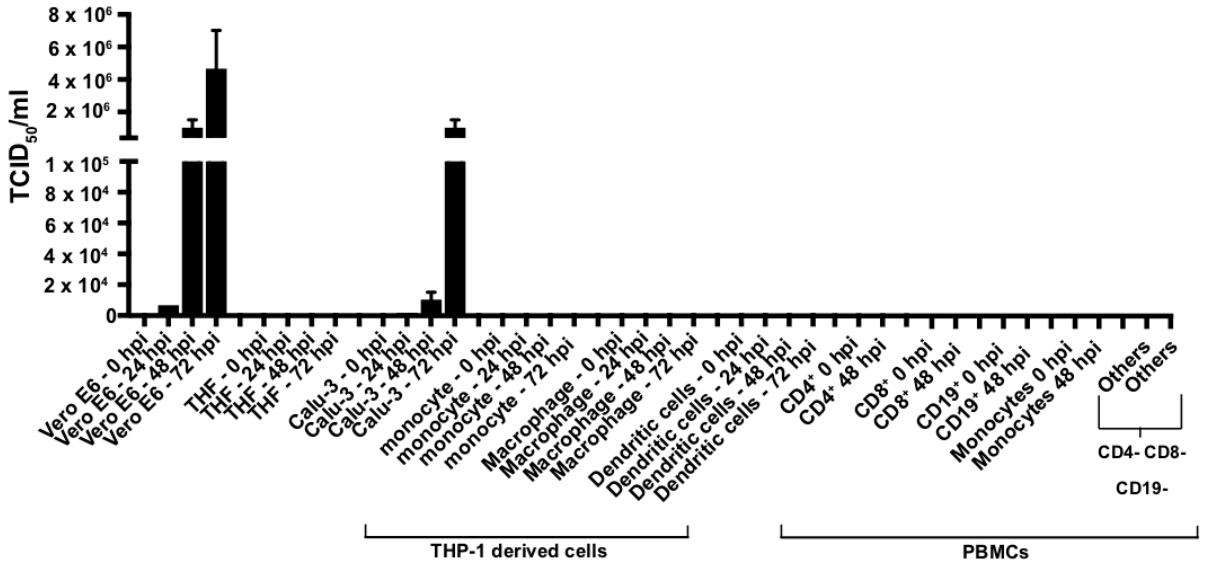

358

359 **Figure 2. Replication of SARS-CoV-2 in human structural and immune cells.** To determine
360 human cells that support SARS-CoV-2 replication, we infected human cell lines and primary
361 cells at an MOI of 0.01 (n = 2 independent experiments; supernatant from each experiment was
362 titrated in triplicates). We infected Vero E6 cells as a control. THF and Calu-3 cells represent

363 human structural cells. THP-1 is a monocyte cell line that was used to derive macrophages and
364 dendritic cells. PBMCs from healthy human donors (n = 2 independent donors) were used to
365 generate $CD4^+$, $CD8^+$, $CD19^+$, monocytes and other ($CD4^-$ $CD8^-$ $CD19^-$) cell populations.
366 Supernatant from infected cells were collected at various times and titrated on Vero E6 cells to
367 determine virus titres ($TCID_{50}$/ml). hpi, hours post infection; CD, cluster of differentiation;
368 PBMC, peripheral blood mononuclear cells.
369

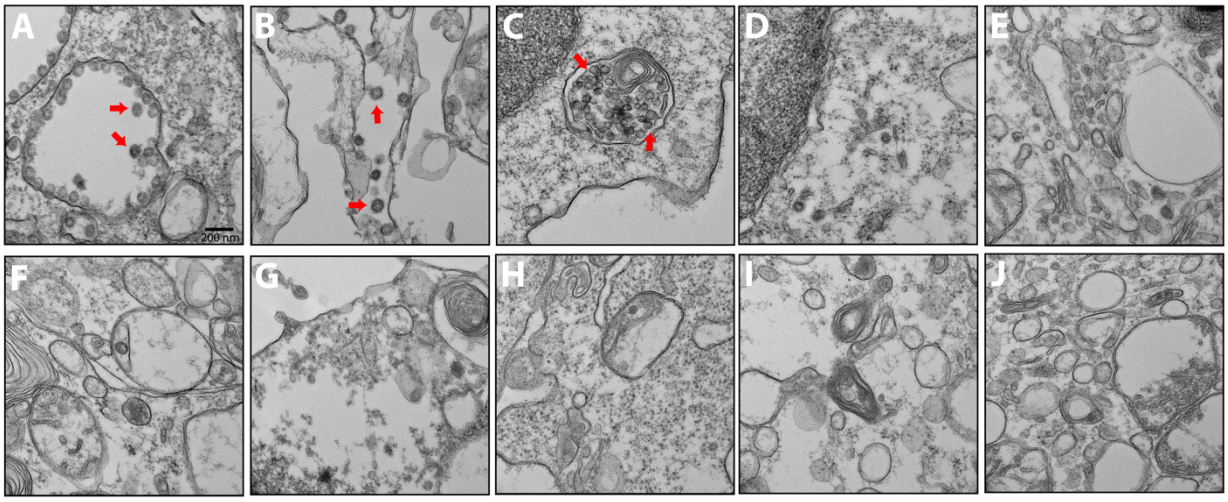

370

371 **Figure 3. Electron micrographs of SARS-CoV-2 infected cells.** To detect coronavirus-like
372 particles in experimentally infected human structural and immune cells, we infected a range of
373 cells with SARS-CoV-2 at a MOI of 0.01 for 48 hours. The cells were fixed, processed and
374 imaged using a transmission electron microscope (n = 10 fields / cell type). Representative image
375 of each cell line is shown above. Virus-like particles are indicated by red arrows. (A) Vero cells.
376 (B) Calu-3 cells. (C) $CD4^+$ PBMC. (D) $CD8^+$ PBMC. (E) $CD19^+$ PBMC. (F) Monocytes from
377 PBMC. (G) Other cells from PBMC ($CD4^-$ $CD8^-$ $CD19^-$ cell populations). (H) THP-1 monocyte.
378 (I) THP-1-derived macrophage. (J) THP-1-derived dendritic cell.
379

380 **TABLE**

Metric or Mutation	SARS-CoV-2/SB2	SARS-CoV-2/SB3_TYAGNC
Number of Paired Reads	730,137 bp	690,167 bp
Reads from SARS-CoV-2	94.0%	94.4%
Number of Assembly Contigs	1	1
Assembly N50	29,494 bp	29,369 bp
Average Depth of Coverage of Reads	7940.0 fold	7550.1 fold
Total Assembly Length	29,494 bp	29,369 bp
SARS-CoV-2 Assembly Completeness	98.6%	98.2%
Unresolved 5' sequence	262 bp	272 bp
Unresolved 3' sequence	200 bp	205 bp
pos. 884 (orf1ab polyprotein)		**R207C (CGT→TGT)**
pos. 1397 (orf1ab polyprotein)	**V378I (GTA→ATA)**	**V378I (GTA→ATA)**
pos. 2832 (orf1ab polyprotein)	K856R (AAG→AGG)	
pos. 3040 (orf1ab polyprotein)		Y925Y (TAC→TAT)
pos. 8327 (or1ab polyprotein)	18.1% of reads suggest L2688F (CTT→TTT)	
pos. 8653 (orf1ab polyprotein)		**M2796I (ATG→ATT)**
pos. 10353 (orf1ab polyprotein)	5.6% of reads suggest K3363T (AAG→ACG)	
pos. 11074 (orf1ab polyprotein)	10.2% of reads suggest +TTT and a deletion between positions 10809 and 13203	
pos. 11083 (orf1ab polyprotein)	**L3606F (TTG→TTT)**	**L3606F (TTG→TTT)**
pos. 25413 (ORF3a protein)		36.7% of reads suggest I7I (ATC→ATT)
pos. 28688 (nucleocapsid phosphoprotein)	**L139L (TTG→CTG)**	**L139L (TTG→CTG)**

381

382 **Table 1. Sequencing read and genome assembly statistics.** Predicted mutations are relative to
383 the MN908947.3 SARS-CoV-2 genome (29,903 bp). Mutations within codons are underlined.
384 All mutations were predicted by 100% of sequencing reads mapping to that position, unless
385 otherwise noted. None of the mutations with support from less than 100% of sequencing reads
386 appeared in the final assembled genome consensus sequences. Substitutions in bold have been
387 observed in direct sequencing of patient isolates associated with travel history to Wuhan and Iran
388 (Mubareka & McArthur, unpublished).
389
390
391
392
393
394
395
396
397
398
399
400
401
402
403
404